Environ. Sci. Technol. 1997, 31, 1419–1425

Selenium Redox Reactions and Transport between Ponded Waters and Sediments

TETSU K. TOKUNAGA*

Earth Sciences Division, E. O. Lawrence Berkeley National Laboratory, 1 Cyclotron Road, Berkeley, California 94720

GORDON E. BROWN, JR.

Department of Geological and Environmental Sciences, Stanford University, 138 Mitchell Building, Stanford, California 94305

INGRID J. PICKERING

Stanford Synchrotron Radiation Laboratory, SLAC, P.O. Box 4349, MS 69, Stanford, California 94309

STEPHEN R. SUTTON

Department of Geophysical Sciences and Consortium for Advanced Radiation Sources, The University of Chicago, 5640 South Ellis Avenue, Chicago, Illinois 60637

SASA BAJT

Lawrence Livermore National Laboratory, P.O. Box 808, L-395, Livermore, California 94550

Understanding the cycling of trace elements such as selenium in the environment requires information on mass transfer and reactions occurring across boundaries. Selenium partitioning and redox transformations in ponded laboratory sediments was compared with a model based on the transport of Se(VI) and Se(IV) between surface waters and sediment pore waters. Waters containing Se(VI) were ponded over initially nonseleniferous sediment columns. X-ray absorption spectroscopy demonstrated Se reduction to Se(0) in these sediments. Synchrotron X-ray microprobe analyses revealed very high Se concentrations within millimeters of the sediment surface. Concentrations of Se(VI) and Se(IV) in sediment pore waters were used as time-dependent boundary conditions to model concentrations of these species in overlying pool waters. Two parameters, the mass transfer coefficient and pool Se(VI) apparent reduction rate constant, were optimized. The successful application of mass transfer coefficients in this study resulted from Se reduction rates within very shallow boundary zones being proportional to Se concentration gradients acting across these zones, rather than solely representing diffusion across these zones. The large gradients in Se concentrations observed in these sediment columns indicate that experimental methods with spatial resolution finer than 1 mm are needed before mechanistic diffusion–redox analyses can be successfully applied to these types of systems.

Introduction

Selenium is both an essential nutrient and a potentially toxic trace element (*1–3*). Its solubility and mobility in the environment are strongly dependent on its valence and specific chemical state. Common inorganic species include soluble selenate [Se(VI)], selenite [Se(IV)], insoluble elemental selenium [Se(0)], and various metal and organic selenides (*4, 5*). Selenite, which is stable under moderately reducing conditions, is soluble but can strongly adsorb onto surfaces of common soil minerals and organic matter (*6–11*). Organoselenium species include seleno-amino acids and volatile methylated Se compounds (*12–15*). The role of microorganisms in catalyzing Se redox transformations of environmental importance is now well-recognized (*2, 3, 14, 16–20*). Knowledge of Se speciation and partitioning within various environmental compartments is important in the evaluation of potential risks arising from deficiency or toxicity (*21, 22*). Wide variations in Se solubility and sorption characteristics among its different forms require that its speciation be understood in order to predict transport between compartments.

Transport across boundaries between surface waters and underlying sediments is important in the cycling of many trace elements (*23*). Portions of the Se cycle in wetlands, lakes, rivers, ocean bottoms, and agricultural drainage water evaporation ponds occur across interfaces between surface waters and sediments (*24, 25*). Selenium transport and transformations in such environments has received considerable attention over the past 10 years since the implication of Se toxicity in wildlife deaths and deformities at Kesterson Reservoir, California (*21, 25–32*).

Investigations of redox-dependent trace element transport require speciation with respect to valence states. Trace element speciation methods for sediments typically rely on selective extraction techniques (*33–35*). Such techniques can introduce uncertainties arising from possible alteration of speciation during extraction procedures (*36–39*). X-ray absorption spectroscopy (XAS) has become established as an analytical method that permits direct speciation of a wide range of elements (*40–43*). The method has been applied to in situ determinations of Se(IV) and Se(VI) adsorption at mineral surfaces (*44, 45*). The valence sensitivity of X-ray absorption near-edge structure (XANES) spectroscopy has been exploited in oxidation state studies of various elements (e.g., refs 46–48). Recently, XAS has been used to determine Se oxidation states in contaminated sediments from Kesterson Reservoir and to track Se reduction in laboratory sediments during flooding (*49–51*). In the present paper, we focus on Se mass transfers across the surface water–sediment boundary in these laboratory systems.

Concentrations of various chemical species at interfaces between surface waters and sediments often change abruptly over very short distances (*23, 52*). Information on chemical concentrations at appropriately high spatial resolution is essential when testing models of chemical transport and transformation in such environments. The synchrotron X-ray fluorescence microprobe (SXRFM) permits two-dimensional mapping of a wide variety of trace elements, with spatial resolution approaching 1 μm (*53, 54*). This tool has recently been used to study small-scale heterogeneity of Se concentrations in contaminated sediments from Kesterson Reservoir (*55*). In the present work, the SXRFM was used at the end of the experiment to obtain a high-resolution Se map within the surface region of a sediment column expected to exhibit large concentration gradients. This spatially resolved information supplemented fluorescence XAS used to determine Se speciation in surface sediments at various times during the course of the experiment.

This study is concerned with Se transport and transformations in shallow, hydrostatically ponded laboratory sedi-

* Corresponding author e-mail: tktokunaga@ibl.gov; phone: (510)-486-7176; fax: (510)486-5686.

S0013-936X(96)00665-7 CCC: $14.00

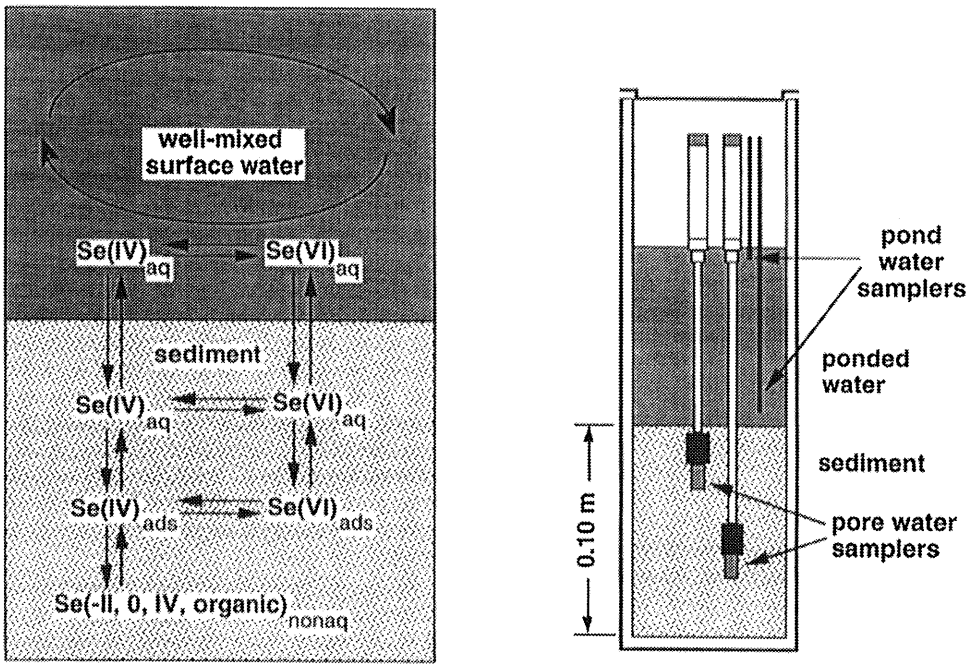

FIGURE 1. (a, left) Conceptual model for Se cycling within the pond–sediment system. (b, right) Experimental column design.

ments. Hydrostatic columns provide simple experimental conditions for evaluating the relative importance of diffusive exchanges of Se species between ponded waters and sediments and Se reduction within ponded waters. They can also represent major features of natural vernal pools as well as ephemeral pools formed over selenium-contaminated sediments of Kesterson Reservoir (*32*). In this study, a simple two-compartment mass transfer model for the exchange of soluble selenate [Se(VI), as SeO_4^{2-}] and selenite [Se(IV), as SeO_3^{2-}] between well-mixed surface waters and shallow sediment pore waters was developed. Measured concentrations of Se(VI) and Se(IV) in sediment pore waters were used to provide time-dependent boundary conditions with which these species exchanged with overlying pool waters. These exchanges were modeled with mass transfer coefficients. First-order reduction of Se(VI) to Se(IV) within ponded waters was included in the model. Mass transfer coefficients and pool Se(VI) reduction rate constants served as adjustable parameters, optimized to provide best model fits to data. The mass transfer coefficients were compared with reasonable values of diffusion coefficients and diffusion lengths for the purpose of testing a diffusion-based interpretation of Se transport between ponded waters and sediments. This study relies on a two-compartment model (pool and sediment) rather than a more comprehensive, multi-compartment reactive transport analysis because of the limited number of experimental sampling locations and a focus on understanding Se removal from ponded waters. We later show that a strictly diffusion-based analysis of exchanges between the pool and surface sediment compartments (both defined by sampling zones) does not account for the important process of Se reduction within the thin boundary zone.

Transport Model

The conceptual model used to account for temporal variations in surface water Se concentrations is shown in Figure 1a. Based upon previous XAS results (*50, 51*), only Se(VI), Se(IV), and Se(0) were included in the systems under consideration. Adsorption of Se(IV) and Se(VI) were not included in model calculations for two reasons. First, in the high concentration ranges used in our experiment, the relative concentrations of potentially adsorbed species is small. Pore water Se concentrations ranged up to 240 g m^{-3}, and total Se concentrations in near-surface sediments were in the range of 100–1000 mg kg^{-1}. Based on previous experiments on this sediment, which indicated Se(IV) adsorption maxima of about 3 mg kg^{-1}, the adsorbed fraction amounts at most to only 0.3–3% of the sediment inventory. Second, in the application of this mass transfer model, the pool–sediment Se transport remains directly proportional to the measured, macroscopic concentration gradients in the solution phase, regardless of sorption or precipitation reactions. Based on measurement of uniform Se concentrations within water columns (described later), the surface waters were approximated as well-mixed compartments. This approximation is likely to be reasonable in shallow vernal pool environments. This study focuses on removal of Se(IV) and Se(VI) from ponded waters and is therefore primarily concerned with their aqueous phase compartments shown in the upper regions of Figure 1.

Information on Se concentrations in sediment pore waters obtained from the shallowest sampler (at the 25 mm depth) in each column was used to predict Se(VI) and Se(IV) exchanges between sediments and ponded waters. These exchanges will first be modeled with mass transfer coefficients (*56*) rather than with diffusion coefficients because the former approach is more general. We later evaluate the adequacy of diffusive transport across a thin boundary layer in accounting for pool–sediment Se exchanges. In the present approach, the mass transfer coefficient for valence state i (equal to VI or IV) is denoted by $k_{Se(i)}$ (L T^{-1}). For a well-mixed pool of constant volume V_p, mass transfer across a pool–sediment interface is described by

$$V_p \frac{\partial [Se(i)]_p}{\partial t} = -A k_{Se(i)} \{[Se(i)]_p - [Se(i)]_s\} \qquad (1)$$

where A is the macroscopic surface area of the pond–sediment interface and the subscripts p and s denote pond and sediment, respectively. Concentrations in both pond waters and sediment pore waters were referenced to a unit volume of the aqueous phase. The above equation accounts only for transport between the two compartments and ignores changes in concentrations of Se(VI) and Se(IV) due to reactions. When reactions within ponded waters are dominated by Se(VI) reduction and when they are treated as being apparent first-order with respect to Se(VI) concentration, then

$$\frac{\partial[\mathrm{Se}(i)]_p}{\partial t} = -\frac{k_{\mathrm{Se}(i)}}{L_p}\{[\mathrm{Se}(i)]_p - [\mathrm{Se}(i)]_s\} \pm k_r[\mathrm{Se(VI)}]_p \quad (2)$$

where L_p denotes the height of the ponded water column ($L_p = V_pA^{-1}$), and k_r is the apparent first-order Se(VI) reduction rate constant. The $+k_r$ and $-k_r$ terms are for Se(IV) production and Se(VI) reduction, respectively. Given initial concentrations of Se(VI) and Se(IV) in the pool waters $[\mathrm{Se}(i)]_{p,0}$ and time-dependent concentrations of these species in sediment waters, eq 2 was numerically integrated to model time-dependent Se(VI) and Se(IV) concentrations:

$$[\mathrm{Se}(i)]_{p,t} = [\mathrm{Se}(i)]_{p,0} + \int_0^t \left\{\frac{-k_{\mathrm{Se}(i)}}{L_p}\{[\mathrm{Se}(i)]_p - [\mathrm{Se}(i)]_s\} \pm k_r[\mathrm{Se(VI)}]_p\right\} dt \quad (3)$$

For this purpose, the sparse set of data on sediment pore water concentrations (collected at 1−11 day intervals) was enhanced via linear interpolation to provide more continuous sediment concentration versus time values (0.5 day intervals). Values of $k_{\mathrm{Se}(i)}$ and k_r were taken as constant for a given simulation and adjusted to provide the best overall fits to data. Although separate $k_{\mathrm{Se}(i)}$ could be applied for Se(IV) and Se(VI) transfers within a given system, only one value was used in order to minimize the number of adjustable parameters. If the Se mass transfers could be accounted for solely by diffusion through a boundary layer, without changes in Se concentrations within this layer, the above equations would have the same form. However, $k_{\mathrm{Se}(i)}$ would be replaced by D_e/L_B, where D_e and L_B are the pond−sediment boundary region effective diffusivity and diffusion length, respectively.

There are some important limitations associated with this procedure. The approach taken amounts to curve-fitting with a minimum number of parameters [2 per system, or 3 if separate $k_{\mathrm{Se}(i)}$ values were used for Se(IV) and Se(VI) mass transfers]. While these parameters are assigned constant values within a given simulation, the factors that they attempt to represent are likely to be time-dependent. The $k_{\mathrm{Se}(i)}$ depend fundamentally upon the effective thickness of the L_B and on time-dependent reactions (both microbially mediated redox and exchange at mineral surfaces) that take place within and beyond this boundary region. The k_r is also expected to be time dependent, especially because of its dependence on microbial population dynamics. On the other hand, the use of constant parameters allows for direct comparisons of the average behavior of different systems. In addition, direct comparisons between $k_{\mathrm{Se}(i)}$ and D_e/L_B can be made later.

In the diffusion-based approach to describing mass transfer between ponded waters and sediments, Se transport is assumed to occur through a diffusion-limited region, described by series resistance (water and water-saturated sediment) diffusivities. Diffusive exchanges were modeled without inclusion of Se reactions (reduction or adsorption) within the boundary layer because of insufficient supporting data. The diffusivity of SeO_4^{2-} in water, in the dilute solution limit, was determined through solution conductance measurements (*56, 57*). This conductance-based diffusivity, $D_o = 1.03 \times 10^{-9}$ m^2 s^{-1}, is close to that reported previously (*57*) for SO_4^{2-} in the dilute limit (1.07×10^{-9} m^2 s^{-1}). The diffusivities of both SeO_3^{2-} and SeO_4^{2-} in higher ionic strength solutions used in this study were assigned values of 1.0×10^{-9} m^2 s^{-1}. Combining this diffusivity with information on sediment porosity f (0.52 in this case) in the empirically based expression for the diffusion coefficient in a sediment:

$$D_s = \alpha f D_o \quad (4)$$

gives $D_s = 29$ mm^2 d^{-1}, when a typical α value of 0.65 is used. Similar D_s values were reported for SO_4^{2-} in sediments in the review by Iversen and Jorgensen (*58*). The series resistance effective diffusivity through the water−sediment boundary layer, D_e, is

$$D_e = (L_w + L_s)\left(\frac{L_w}{D_o} + \frac{L_s}{D_s}\right)^{-1} \quad (5)$$

where L_w and L_s represent diffusion lengths in the water and sediment segments, respectively. L_w is the vertical distance from the sediment−pond interface up to the lowest region of the ponded water that sustains well-mixed solute concentrations. L_s is taken as the distance from the sediment−pond interface downwards to the region in the sediment at which aqueous Se concentrations are equal to those obtained in the shallowest sediment water sampler. The sum of these two lengths is defined as the boundary layer thickness, L_B. In the analyses to follow, modeling of time trends for solution Se concentrations in a given system will only permit direct evaluation of the pond−sediment mass transfer coefficient ($k_{\mathrm{Se}(i)}$), which is equal to the quotient D_e/L_B only when changes in Se concentrations within L_B are minor. From eqs 4 and 5, we have

$$\frac{D_e}{L_B} = \frac{D_o}{L_w + \left(\frac{L_s}{\alpha f}\right)} \quad (6)$$

This result will be used later when magnitudes of L_s are compared for two systems with very different rates of Se removal from ponded waters.

Materials and Methods

Laboratory sediment columns were designed to study Se reduction within sediments following ponding with seleniferous waters. A previously completed part of this study involved applications of XAS to determine changes in oxidation states of Se (*49−51*). Sediments for these columns were collected from Kesterson National Wildlife Refuge in an area with no previous history of exposure to seleniferous waters. The general chemical composition of these sediments has been described previously (*35, 59*). The total Se concentrations in the sampled sediment was <0.5 mg kg^{-1}. Homogenized sediments were packed (while still at a field-moist water content of 0.178 kg kg^{-1}) to a depth of 100 mm in 4 PVC columns (76.5 mm i.d.) and to an equivalent dry bulk density of 1.28 Mg m^{-3} (Figure 1b). The total porosity and initial water-filled porosity were 0.52 and 0.23, respectively. The column bottoms were sealed, and the walls were sufficiently tall to permit ponding above the sediments. Two of the columns (denoted C1 and C3) were uniformly packed with soil. The other two columns (denoted C2 and C4) were amended with cuttings of *Bromus mollis* leaves and stems added to the uppermost 30 mm of soil in order to observe possible influences of decomposing vegetation on Se reduction. The mass of organic matter added in this manner amounted to an air-dry equivalent of 0.2 kg m^{-2} (1.03 g per column), which corresponds to a typical quantity of annual grass biomass produced at the field site. Soil water samplers were embedded at 25 and 75 mm below the sediment surface in one unamended (C3) and one organic matter amended (C4) sediment column.

Waters with an initial Se concentration of 240 g m^{-3} (3.0 mM) were ponded over these previously uncontaminated sediments. These initial aqueous Se concentrations are about 10^3 times higher than typical values observed in the agricultural drainage waters ponded at Kesterson Reservoir. Laboratory experiments were conducted with elevated Se concentrations in order to assure collection of high quality X-ray absorption spectra on sediments. Pond water and sediment pore water samples were periodically collected to obtain information on Se concentrations and concentration

gradients across the water–sediment boundary. The first complete set of samples, collected within 3 h after ponding, established the initial conditions for the later mass transfer calculations. Water and sediment sampling and chemical analyses are discussed in greater detail in the earlier studies (*49–51*). Selenium was added to the laboratory solution as 98% Se(VI) (from Na_2SeO_4) and 2% Se(IV) (from Na_2SeO_3). This ratio of Se(VI) to Se(IV) was similar to typical agricultural drain waters that were discharged into Kesterson Reservoir. Analysis of Se in ponded waters and sediment waters was routinely performed by hydride-generation atomic absorption spectrometry (*60*). Occasional total solution Se analyses were also performed by inductively coupled plasma spectrometry. Comparisons between these two spectrometric methods, along with XAS results, showed that Se(VI) and Se(IV) were the only aqueous Se species occurring at significant concentrations in these experiments. The major ion composition of the laboratory solution was designed to resembled that of the agricultural drain waters, dominated by Na^+, SO_4^{2-}, and Cl^-. Ponding with seleniferous water was established by dispensing 550 mL of solution over the sediment surface over about a 1-min interval. This volume corresponded to an equivalent water column 120 mm deep. Upon dispensing the solutions, each column contained an initial ponding depth of 90 ± 3 mm, indicating that the sediment profiles were near saturation (101 ± 10%).

Ponded waters in columns were disturbed as little as possible in an attempt to discern the development of gradients in Se concentrations and speciation within the static water columns. Samples of ponded waters were collected at two depths: one at about 7 mm below the water–air interface and a second sample at about 7 mm above the sediment–water interface, via 1 mm i.d. polyethylene tubing attached to a syringe. Solution sample masses were kept small, ranging from 50 to 200 mg, in order to minimize disturbances to columns. Pond water sampling intervals ranged from daily (initially) up to 14 days toward the end of the ponded phase. Sediment pore water samples were also collected during the 48–51-day ponding period.

Methylated Se will not be considered in this study since the alkaline H_2O_2 traps for collection of gaseous Se (*60*) included in this experiment showed that less than 0.5% of the total Se inventory was volatilized (*51*). The experiment was terminated after about 50 days of ponding. Depth profiles of total Se were measured by energy-dispersive X-ray fluorescence (*61*). Surface soil Se was analyzed by XAS at Stanford Synchrotron Radiation Laboratory several times at the beginning of ponding and at the end of the experiment. A sample of surface sediment from the C4 column was also analyzed for Se with the SXRFM at the National Synchrotron Light Source in order to obtain depth profiles of total Se with high spatial resolution (0.25 mm vertical step sizes).

Results and Discussion

Experimental. Similar time trends in surface water Se composition were observed within the duplicate columns. Considerably different trends in surface water Se concentrations were observed between columns with and without surface sediment organic matter additions. Since only one column from each of the two treatments was instrumented with pore water samplers, only these instrumented systems (C3 and C4) will be considered in detail. Depth profiles combining data on Se(VI) in ponded waters and in sediment pore waters for several different times are shown in Figures 2a (unamended C3) and 3a (organic matter amended C4). Depth profiles for aqueous phase Se(IV) for these same times are presented in Figures 2b and 3b. As a result of infiltration ponding waters into initially unsaturated sediments, the pore water Se concentrations collected from shallow depths at near time zero (1.4 days) are similar to those of the ponded waters. In both systems, surface water Se(VI) concentrations

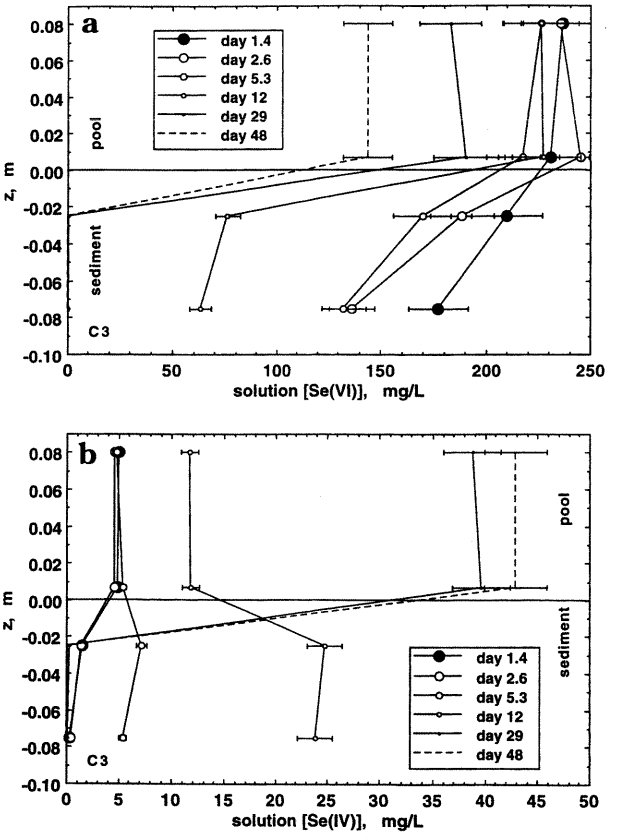

FIGURE 2. Depth profiles of total dissolved Se(VI) (a) and Se(IV) (b) in unamended columns, combining ponded waters and sediment pore waters.

declined over time, while Se(IV) concentrations increased for at least some portion of the ponded period. Net decreases in total dissolved Se occurred in surface waters of both systems, with more rapid declines in systems with organic matter added to surface sediments. No significant gradients in concentrations of the Se species were detectable within the ponded water columns. These observations support describing the ponded waters as well-mixed volumes. Furthermore, while the sampling tube was placed vertically downwards to about 7 mm above the pool–sediment interface during collections, the sampled volumes may have extended 1–2 mm closer toward the sediment. Thus, the diffusion boundary layer above the sediment, over which significant gradients in Se concentrations could occur, is probably less than 7 mm in thickness.

More rapid rates of Se reduction occur within the sediments than in the ponded waters. The XAS study showed Se(VI) reduced sequentially from Se(IV) to Se(0) during ponding, with Se(0) occurring as early as 3.8 days after flooding in the amended sediments (*49–51*). By the end of the experiment, 25% of the original Se in the surface waters was transported into unamended sediments. For systems amended with organic matter, 95% of the Se originally in ponded waters was transported into the sediments. Accumulations of Se within sediments were largely confined to the near-surface regions (<25 mm depth) in each type of column (*51*). The onset of reducing conditions is expected to occur earlier in surface sediments than in deeper sediments of both types of systems because of some soil air displacement and entrapment in the column bottoms. This process would provide a residual supply of O_2 in the deeper portions of the columns. In addition, columns with surface sediments amended with readily reducible organic carbon would be expected to become anaerobic more rapidly. Reducing conditions in surface sediment promoted Se(VI) reduction to Se(IV) and to Se(0), allowing a net accumulation of insoluble

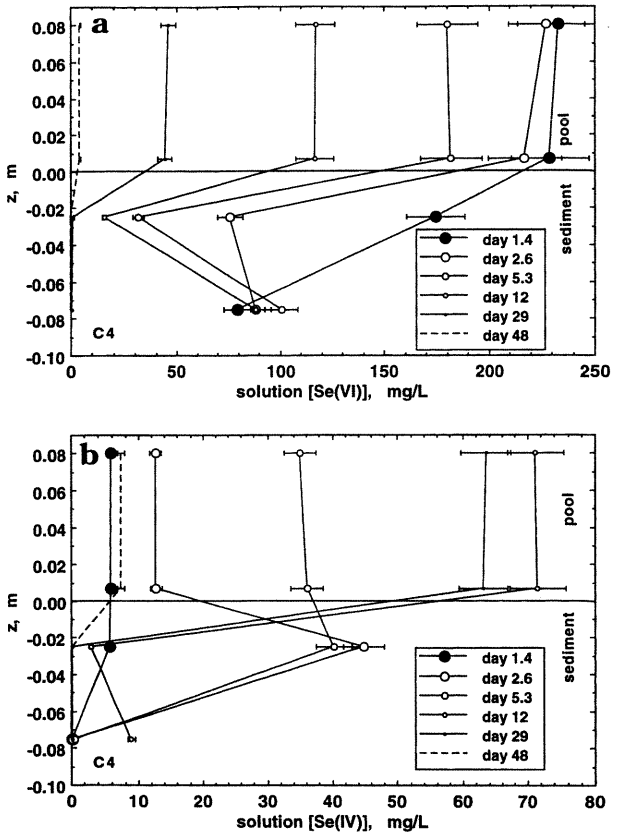

FIGURE 3. Depth profiles of total dissolved Se(VI) (a) and Se(IV) (b) in columns amended with organic matter, combining ponded waters and sediment pore waters.

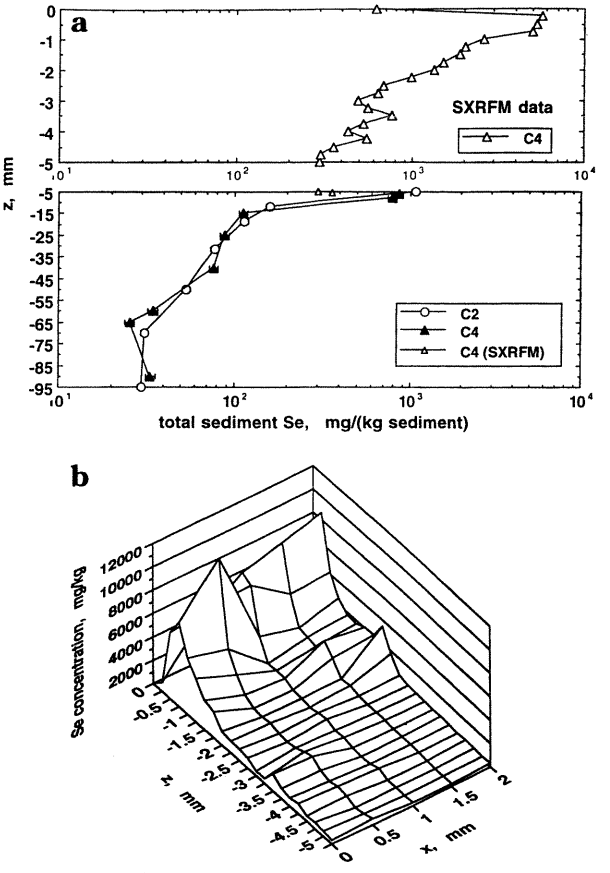

FIGURE 4. Total Se concentration profiles in sediment samples analyzed at the end of the ponding experiment (sediments amended with organic matter within the upper 30-mm region). (a) Lower profile from conventional XRF and SXRFM (lower panel), upper profile average from SXRFM (upper panel), and (b) two-dimensional SXRFM map of Se within a surface sediment sample from the amended column.

Se species (*49*–*51*). From Figure 4a, it appears that the organic matter amended sediments become extremely reducing at the interface with ponded waters. The procedure used to sample the columns permitted only relatively coarse spatial resolution (5–10 mm along the vertical column) in the conventional XRF analyses for Se. In view of the highly skewed distribution of Se in the coarser scale XRF analyses of the organic matter amended sediment, a higher resolution map of a surface subsample was obtained with SXRFM. The SXRFM map was performed over a 2 mm wide, 5 mm long, vertical slice of the surface sediment. The vertical and horizontal steps were taken in 0.25- and 0.50-mm increments, respectively. Horizontally averaged (over the 2 mm width) total Se profiles are included in Figure 4a. These data show that the highest accumulations of Se occur within the top 1 mm of this column, indicative of rapid reduction of Se to Se(0). The two-dimensional SXRFM map of Se concentrations in this surface sediment is shown in Figure 4b. Heterogeneities in total Se concentrations along the horizontal direction are also evident in this representation, although these are not as varied as the vertical heterogeneities.

Mass Transfer Model. The two adjustable parameters, the mass transfer coefficient $k_{Se(i)}$ and the rate constant k_r, were varied in order to determine optimum values (least sums of squared differences between data and models) for matching measured pool Se(VI) and Se(IV) concentrations. Best-fit results for modeling Se(VI) and Se(IV) concentrations in pools over the two sediment types are shown in Figure 5a,b along with several other trial curves. In the case of the unamended sediment, the $k_{Se(i)}$ that yielded the best fits without using a reduction rate constant were in the range of 0.80–0.93 mm d^{-1}. While these fits matched the time dependence of $[Se(VI)]_p$ quite well, the buildup in $[Se(IV)]_p$ with time was significantly underestimated (Figure 5a). Both time trends in $[Se(VI)]_p$ and $[Se(IV)]_p$ were well matched [$r^2 = 0.957$ and 0.960 for Se(IV) and Se(VI), respectively] by setting $k_{Se(i)}$ = 0.80 mm d^{-1} and by assigning a value of 4×10^{-3} d^{-1} to k_r. For the system amended with organic matter (Figure 5b), the optimum matches were obtained with $k_r = 3 \times 10^{-2}$ d^{-1}. Best matches [$r^2 = 0.894$ and 0.986 for Se(IV) and Se(VI), respectively] for both $[Se(VI)]_p$ and $[Se(IV)]_p$ time trends in the amended system were obtained with $k_{Se(i)} = 4.0$ mm d^{-1}. Thus, mass transfer of both Se species from ponded waters into sediments occurs five times more rapidly in the columns with organic matter amendments added to the sediment surface. Note also that Se(VI) reduction within ponded waters occurs about eight times faster in the amended system. The fact that a significantly large k_r was needed to match data in C4 than in C3 shows that other important factors in pool waters differed between these two systems. The plausible factors are higher concentrations of easily reducible organic carbon and of selenium-reducing bacteria in the waters ponded over the amended C4 columns. Diffusive release of organic matter from sediments into water columns, dynamics of microbial growth, and biochemistry of Se reduction are beyond the scope of this study.

The optimized $k_{Se(i)}$ values can be combined with data on gradients of [Se(VI)] and [Se(IV)] at the pond–sediment boundaries to calculate fluxes of these species. Transport rates and cumulative mass transfers are obtained through eq 1 and its numerical integration, respectively. Results of these calculations for the unamended system show transport dominated by Se(VI) at all times. By the end of the experiment, only 11% of the Se transport into the sediment occurred in the Se(IV) form. Mass transfer calculations on the amended system show very different behavior. The initial mass transfer rate for Se(VI) into sediments becomes very large within the

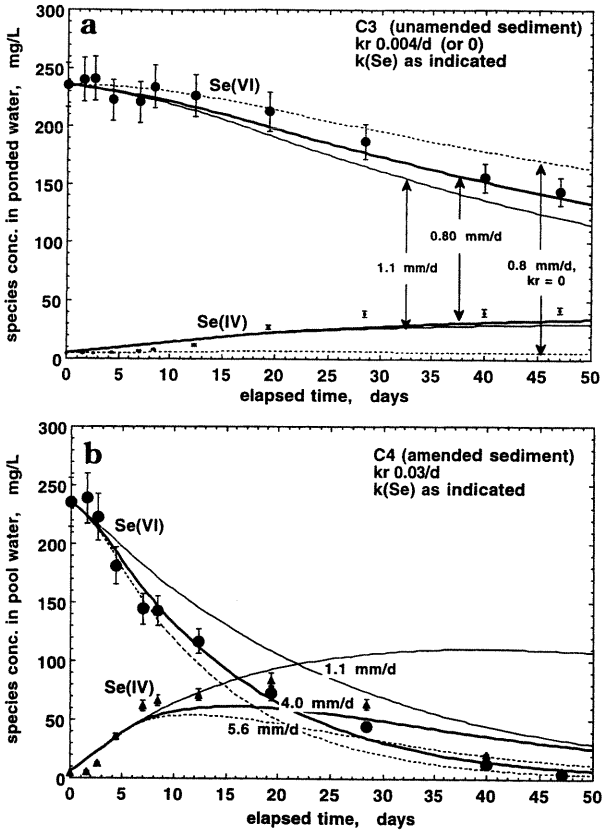

FIGURE 5. Time trends for measured pool water Se(VI) and Se(IV) concentrations (data points) and modeled results (curves) for (a) unamended sediments, and (b) sediments amended with organic matter.

first 5 days and then gradually diminishes over the remainder of the experiment. A significant transfer of Se(IV) from shallow sediment pore waters back into surface waters is also predicted between days 2 and 6, followed by a long period of Se(IV) transport from surface waters back into sediments. Transport from sediments back into ponded waters are predicted whenever concentrations of a particular species are higher in shallow pore waters than in the pond. The fact that such behavior is predicted only for Se(IV) results from more rapid Se(VI) reduction in sediments than in ponded waters. Calculations also indicate that about 43% of the Se mass transfer into the amended sediment occurred through Se(IV) transport.

The feasibility of accounting for the pond–sediment mass transfer solely by diffusion through a boundary layer was tested by assigning the optimized values of $k_{Se(i)}$ to D_e/L_B for each system. Thus, the unamended and amended columns have D_e/L_B values of 0.80 and 4.0 mm d^{-1}, respectively. In order to test the diffusion boundary model for exchanges between ponded waters and shallow sediments, it will be useful to determine the surface sediment diffusion length L_s. Although the shallowest sediment water samplers were centered at 25 mm below the interface, it is conceivable that the sampled solution chemistry is representative of a different or wider depth range. Together with known or well-constrained approximate values of D_o, α, and f, we have two equations (in the form of eq 6) with four unknowns (the L_w and L_s for the two cases). It is reasonable to equate the L_w in the unamended system to that in the amended system. Using previously noted values, this leads to L_s(unamended) = L_s (amended) + 29 mm. The physical constraint that the diffusion boundary layer in the ponded waters must occur below the deepest point of pool sampling requires that $0 < L_w < 7$ mm. This in turn leads to the conclusion that L_s(unamended) = 35 ± 1 mm and L_s(amended) = 6 ± 1 mm. The diffusion boundary layer model thus leads to calculated values of L_s that are inconsistent with the location of the shallow pore water samplers.

In this simple diffusion boundary layer model, the region within L_s (and for that matter within L_B) serves only to transport mass from one region into another and does not allow for local mass accumulation. However, such a conceptualization is clearly inconsistent with data on the vertical distribution of Se within these columns (Figure 4). The bulk sediment analyses by conventional XRF showed that most of the Se was concentrated within the upper 30 mm of the C3 sediment and within the upper 10 mm in the C4 sediment. Therefore, the successful fits achieved with the mass transfer coefficients do not result from diffusive transport across the region over which aqueous phase concentration gradients were measured. Instead, Se immobilization within this zone was proportional to these concentration gradients. XAS showed that insoluble Se(0) accounts for more than 90% of the Se in this zone. Higher resolution analyses by SXRFM on a C4 sediment sample showed maximum Se reduction and accumulation within less than 1 mm of the interface with ponded waters. These data collectively show that the Se reduction and accumulation within the short distance (25 mm) between the sediment surfaces and the shallowest pore water samplers account for most of the Se removed from the ponded waters and that large concentration gradients occur in this boundary region.

Comparisons of data and model results from these two types of columns show that the depths associated with Se reduction and diffusion-limited transport within sediments of shallow aquatic systems can strongly influence trends in surface water quality. These findings can be useful in understanding trends in ephemeral pool water quality in trace element-contaminated environments. More generally, the extremely surficial localization of Se reduction and accumulation can have important implications on the cycling of this trace element in aquatic ecosystems. The extremely large gradients in Se and the reduction of Se within this short boundary region show that higher spatial resolution in Se concentrations and speciation are required in order to support mechanistic transport models of these systems. The combined use of XANES and SXRFM, referred to as micro-XANES, is now being applied to obtain valence-specific maps of different oxidation states of particular trace elements (*62*, *63*). Recently, investigations have been initiated to apply micro-XANES to real-time tracking of redox-dependent transport and reactions of Se and Cr in sediment systems (*62*).

Acknowledgments

We thank George Parks, John Bargar, Singfoong Cheah, Andrea Foster, Ping Liu, Maria Peterson, Hillary Thompson, and Ning Xu of Stanford University for help with data collection; P. Frank and S. Shadle for assistance in obtaining Se standards; and Graham George for helpful discussions and access to his XAS edge-fitting software. We thank Robert Giauque, Andy Yee, and Dan Phillips of Lawrence Berkeley National Laboratory for providing chemical analyses and the staff at Stanford Synchrotron Radiation Laboratory and the National Synchrotron Light Source (NSLS) for beamline support. Review comments on this manuscript by Sally Benson and Peter Zawislanski (LBNL), Mavrik Zavarin (University of California, Berkeley), and two anonymous reviewers are greatly appreciated. Research was in part carried out at the NSLS, Brookhaven National Laboratory, which is supported by the U.S. Department of Energy, Division of Material Sciences and Division of Chemical Sciences. T.K.T. acknowledges Sally M. Benson and Tom McEvilly of LBNL for encouragement in developing this study and funding through the Director, Office of Energy Research, Office of Basic Energy Sciences, Geosciences Program of the Department of Energy, under

Contract DE-AC03-76SF00098, and the Laboratory Directed Research and Development Program of LBNL. G.E.B. and I.J.P. acknowledge support through DOE Grant DE-FG03-93ER14347-A000. S.R.S. and S.B. acknowledge support from U.S. Department of Energy Contracts DE-FG02-92BR14244-(SRS) and DE-AC02-76CH00016. Stanford Synchrotron Radiation Laboratory is operated by the DOE, Office of Basic Energy Sciences. The SSRL Biotechnology Program is supported by the NIH, Biomedical Research Technology Program, Division of Research Resources. Further support was provided by the DOE, Office of Health and Environmental Research.

Literature Cited

(1) Rosenfeld, I.; Beath, O. A. *Selenium Geobotany, Biochemistry, Toxicity, and Nutrition*; Academic Press: New York, 1964.
(2) *Selenium in Agriculture and the Environment*; Jacobs, L. W., Ed.; SSSAJ Special Publication No. 23, American Society of Agronomy: Madison, WI, 1989.
(3) *Selenium in the Environment*; Frankenberger, W. T., Jr.; Benson, S. M., Eds.; Marcel Dekker, Inc.: New York, 1994.
(4) Elrashidi, M. A.; Adriano, D. C.; Workman, S. M.; Lindsay, W. *Soil Sci.* **1987**, *144*, 141–152.
(5) Masscheleyn, P. H.; Delaune, R. D.; Patrick, W. H., Jr. *Environ. Sci. Technol.* **1990**, *24*, 91–96.
(6) Geering, H. R.; Cary, E. E.; Jones, L. H. P.; Allaway, W. H. *Soil Sci. Soc. Am. Proc.* **1968**, *32*, 35–40.
(7) Hingston, F. J.; Posner, A. M.; Quirk, J. P. *Faraday Soc. Disc.* **1971**, *52*, 334–342.
(8) Balistrieri, L. S.; Chao, T. T. *Soil Sci. Soc. Am. J.* **1987**, *51*, 1145–1151.
(9) Bar-Yosef, B.; Meek, D. *Soil Sci.* **1987**, *144*, 11–19.
(10) Neal, R. H.; Sposito, G.; Holtzclaw, K. M.; Traina, S. J. *Soil Sci. Soc. Am. J.* **1987**, *51*, 1161–1165.
(11) Christensen, B. T.; Bertelsen, F.; Gissel-Nielsen, G. *J. Soil Sci.* **1989**, *40*, 641–647.
(12) Reamer, D. C.; Zoller, W, H. *Science (Washington, D.C.)* **1980**, *208*, 500–502.
(13) Zieve, R.; Peterson, P. J. *Sci. Total Environ.* **1981**, *19*, 277–284.
(14) Doran, J. W. *Adv. Microb. Ecol.* **1982**, *6*, 1–32.
(15) Thompson-Eagle, E. T.; Frankenberger, W. T., Jr. *J. Environ. Qual.* **1989**, *19*, 125–131.
(16) Zehr, J. P.; Oremland, R. S. *Appl. Environ. Microbiol.* **1987**, *53*, 1365–1369.
(17) Macy, J. M.; Michel, T. A.; Kirsch, D. G. *FEMS Microbiol. Lett.* **1989**, *61*, 195–198.
(18) Oremland, R. S.; Hollibaugh, J. T.; Maest, A. S.; Presser, T. S.; Miller, L. G.; Culbertson, C. W. *Appl. Environ. Microbiol.* **1989**, *55*, 2333–2343.
(19) Oremland, R. S.; Steinberg, N. A.; Maest, A. S.; Miller, L. G.; Hollibaugh, J. T. *Environ. Sci. Technol.* **1990**, *24*, 1157–1164.
(20) Lortie, L.; Gould, W. D.; Rajan, S.; McCready, R. G. L.; Cheng, K.-J. *Appl. Environ. Microbiol.* **1992**, *58*, 4042–4044.
(21) Ohlendorf, H. M. In *Selenium in Agriculture and the Environment*; Jacobs, L. W., Ed.; Soil Science Society of American Special Publication 23; American Society of Agronony: Madison, WI, 1989; pp 133–177.
(22) Luoma, S. N.; Johns, C.; Fisher, N. S.; Steinberg, N. A.; Oremland, R. S.; Reinfelder, J. R. *Environ. Sci. Technol.* **1992**, *26*, 485–491.
(23) Santschi, P.; Hohener, P.; Benoit, G.; Bucholtz-ten-Brink, M. *Mar. Chem.* **1990**, *30*, 269–315.
(24) Cutter, G. A.; Bruland, K. W. *Limnol. Oceanogr.* **1984**, *29*, 1179–1192.
(25) Weres, O.; Jaouni, A.-R.; Tsao, L. *Appl. Geochem.* **1989**, *4*, 543–563.
(26) Presser, T. S.; Barnes, I. U. S. Geol. Surv. **1985**, Water-Resources Investigations Report 84–4220. Menlo Park, CA.
(27) Gilliom, R. J. *Water Resour. Invest. (U.S. Geol. Surv.)* **1989**, *No. 88-4186*.
(28) Long, R. H. B.; Benson, S. M.; Tokunaga, T. K.; Yee, A. *J. Environ. Qual.* **1990**, *19*, 302–311.
(29) Benson, S. M.; White, A. F.; Halfman, S.; Flexser, S.; Alavi, M. *Water Resour. Res.* **1991**, *27*, 1071–1084.
(30) White, A. F.; Benson, S. M.; Yee, A., W.; Wollenberg, H. A., Jr.; Flexser, S. *Water Resour. Res.* **1991**, *27*, 1085–1098.
(31) Tokunaga, T. K.; Zawislanski, P. T.; Johannis, P. W.; Benson, S.; Lipton, D. S. Field investigations of selenium speciation, transformation, and transport in soils from Kesterson Reservoir and Lahontan Valley. In *Selenium in the Environment*; Frankenberger, W. T., Jr., Benson, S., Eds.; Marcel Dekker, Inc.: New York, 1994.
(32) Tokunaga, T. K.; Benson, S. M. *J. Environ. Qual.* **1992**, *21*, 246–251.
(33) Chao, T. T.; Sanzolone, R. F. *Soil Sci. Soc. Am. J.* **1989**, *53*, 385–392.
(34) Lipton, D. S. Ph.D. Dissertation, University of California, Berkeley, 1991.
(35) Tokunaga, T. K.; Lipton, D. S.; Benson, S. M.; Yee, A. W.; Oldfather, J. M.; Duckart, E. C.; Johannis, P. W.; Halvorsen, K. E. *Water Air Soil Pollut.* **1991**, *57–58*, 31–41.
(36) Kheboian, C.; Bauer, C. F. *Anal. Chem.* **1987**, *59*, 1417–1423.
(37) Gruebel, K. A.; Davis, J. A.; Leckie, J. O. *Soil Sci. Soc. Am. J.* **1988**, *52*, 390–397.
(38) Beckett, P. H. T. *Adv. Soil Sci.* **1989**, *9*, 143–176.
(39) Belzile, N.; Lacomte, P.; Tessier, A. *Environ. Sci. Technol.* **1989**, *23*, 1015–1020.
(40) Brown, G. E., Jr.; Calas, G.; Waychunas, G. A.; Petiau, J. *Rev. Mineral.* **1988**, *18*, 431–512.
(41) Koningsberger, D. C.; Prins, R. *X-ray Absorption: Principles, Applications, Techniques of EXAFS, SEXAFS and XANES*; John Wiley and Sons: New York, 1988.
(42) Brown, G. E., Jr.; Parks, G. A. *Rev. Geophys.* **1989**, *27*, 519–533.
(43) Schulze, D. G.; Bertsch, P. M. *Adv. Agron.* **1995**, *55*, 1–66.
(44) Hayes, K. F.; Roe, A. L.; Brown, G. E., Jr.; Hodgsen, K. O.; Leckie, J. O.; Parks, G. A. *Science (Washington, D.C.)* **1987**, *238*, 783–786.
(45) Manceau, A.; Charlet, L. *J. Colloid Interface Sci.* **1994**, *168*, 87–93.
(46) Waychunas, G. A.; Apted, M. J.; Brown, G. E., Jr. *Phys. Chem. Miner.* **1983**, *10*, 1–9.
(47) George, G. N.; Gorbaty, M. L. *J. Am. Chem. Soc.* **1989**, *111*, 3182–3186.
(48) Vairavamurthy, A.; Manowitz, B.; Zhou, W.; Jeon, Y. In *Environmental Geochemistry of Sulfur Oxidation*, Alpers; C. N., Blowes, D. W., Eds.; American Chemical Society Symposium Series 550; ACS: Washington, DC, 1994; pp 412–430.
(49) Pickering, I. J.; Brown, G. E., Jr.; Tokunaga, T. K. In *Stanford Synchrotron Radiation Laboratory 1993 Activity Report*; Stanford University: Stanford, CA, 1994.
(50) Pickering, I. J.; Brown, G. E., Jr.; Tokunaga, T. K. *Environ. Sci. Technol.* **1995**, *29*, 2456–2459.
(51) Tokunaga, T. K.; Pickering, I. J.; Brown, G. E., Jr. *Soil Sci. Soc. Am. J.* **1996**, *60*, 781–790.
(52) Davison, W.; Zhang, H.; Grime, G. W. *Environ. Sci. Technol.* **1994**, *28*, 1623–1632.
(53) Jones, K. W.; Gordon, B. M. *Anal. Chem.* **1989**, *61*, 341A–358A.
(54) Sutton, S. R.; Rivers, M. L.; Bajt, S.; Jones, K. W. *Nucl. Instrum. Methods* **1993**, *B75*, 553–558.
(55) Tokunaga, T. K.; Sutton, S. R.; Bajt, S. *Soil Sci.* **1994**, *158*, 421–434.
(56) Cussler, E. L. *Duffusion: Mass Transfer in Fluid Systems*; Cambridge University Press: Cambridge, 1984.
(57) Robinson, R. A.; Stokes, R. H. *Electrolyte Solutions*; Academic Press: New York, 1959.
(58) Iverson, N.; Jorgensen, B. B. *Geochim. Cosmochim. Acta* **1993**, *57*, 571–578.
(59) Manning, B. A.; Burau, R. G. *Environ. Sci. Technol.* **1995**, *29*, 2639–2646.
(60) Weres, O.; Cutter, G. A.; Yee, A.; Neal, R.; Moehser, H.; Tsao, L. Section 3500-Se. In *Standard Methods for the Examination of Water and Wastewater*, 17th ed.; Clesceri, L. S., Ed.; American Public Health Association: Washington, DC, 1989; pp 3-128–3-141.
(61) Giauque, R. D.; Garrett, R. B.; Goda, L. Y. *Anal. Chem.* **1976**, *49*, 1012–1017.
(62) Sutton, S. R.; Bajt, S.; Delaney, J.; Schulze, D.; Tokunaga, T. *Rev. Sci. Instrum.* **1995**, *66*, 1464–1467.
(63) Bajt, S.; Clark, S. B.; Sutton, S. R.; Rivers, M. L.; Smith, J. *Anal. Chem.* **1993**, *65*, 1800–1804.

Received for review July 31, 1996. Revised manuscript received December 20, 1996. Accepted January 14, 1997.[⊗]

ES960665U

[⊗] Abstract published in *Advance ACS Abstracts,* March 15, 1997.